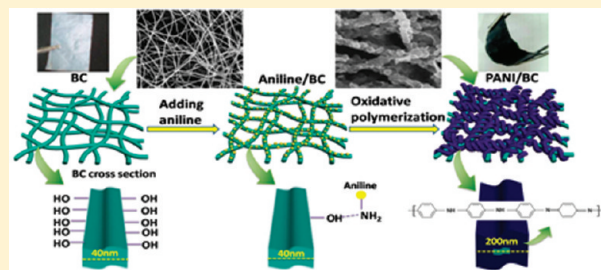


# Flexible Electrically Conductive Nanocomposite Membrane Based on Bacterial Cellulose and Polyaniline

Weili Hu, Shiyan Chen,\* Zhenhua Yang, Luting Liu, and Huaping Wang\*

State Key Laboratory for Modification of Chemical Fibers and Polymer Materials, The Key Laboratory of High-Performance Fiber and Product, Ministry of Education, College of Materials Science and Engineering, Donghua University, Shanghai, 201620, P R China

**ABSTRACT:** The novel conductive polyaniline/bacterial cellulose (PANI/BC) nanocomposite membranes have been synthesized in situ by oxidative polymerization of aniline with ammonium persulfate as an oxidant and BC as a template. The resulting PANI-coated BC nanofibrils formed a uniform and flexible membrane. It was found that the PANI nanoparticles deposited on the surface of BC connected to form a continuous nanosheath by taking along the BC template, which greatly increases the thermal stability of BC. The content of PANI and the electrical conductivity of composites increased with increasing reaction time from 30 to 90 min, while the conductivity decreased because of the aggregation of PANI particles by further prolonging the reaction time. In addition, the acids remarkably improve the accessibility and reactivity of the hydroxyl groups of BC. The results indicate that the composites exhibit excellent electrical conductivity (the highest value was  $5.0 \times 10^{-2}$  S/cm) and good mechanical properties (Young's modulus was 5.6 GPa and tensile strength was 95.7 MPa). Moreover, the electrical conductivity of the membrane is sensitive to the strain. This work provides a straightforward method to prepare flexible films with high conductivity and good mechanical properties, which could be applied in sensors, flexible electrodes, and flexible displays. It also opens a new field of potential applications of BC materials.



## INTRODUCTION

It is well-known that polyaniline (PANI) is a conjugated polymer with interesting properties such as good environmental stability, high electrical conductivity, facile synthesis, and low synthesis costs.<sup>1</sup> It has been used in different applications including sensors, the biomedical field, electronics, electrochromic devices, and fuel cells.<sup>2–7</sup> However, the application of PANI is restricted by the relatively poor mechanical properties. To solve this problem, considerable work has been done in recent years to develop various polymers with good mechanical and processing properties to prepare PANI composites. A variety of polymeric materials with excellent physical properties have been used as good supports for PANI, such as cellulose, rubber, plastic, and textile.<sup>8–12</sup> Among them, cellulose and cellulose derivatives as abundant renewable eco-friendly materials have drawn more and more attention.<sup>1,13</sup> However, natural fibers are composed of only 55–65% cellulose where the isolation and purification of fibers are needed. Besides, the current environmental issues show a pressing need for innovative, sustainable, and recyclable materials with performance at the same level or better than conventional natural fibers.

Bacterial cellulose (BC) is a straight chain polysaccharide with the same chemical structure as cellulose. However, compared with plant-based cellulosic fibers, BC with an ultrafine nanosized three-dimensional fibrous network structure offers many attractive properties. Its fibrils have diameters between 10 and 100 nm with a high crystallinity ( $\sim 90\%$ ), and it also has a highly hydrophilic characteristic due to the many hydroxyl groups on

the surface.<sup>14</sup> Besides, the mechanical properties of BC are much better than those of conventional natural fibers. The Young's modulus and tensile strength reported have reached 20.8 GPa and 357.3 MPa, respectively.<sup>15</sup> Due to these characteristics, some researchers have done many investigations on BC reinforced polymer composites such as cellulose acetate butyrate composites, phenol formaldehyde composites, acrylic resin, and epoxy resin composites.<sup>16–18</sup>

In this paper, PANI/BC conductive nanocomposite membranes have been successfully fabricated by oxidative polymerization of aniline using ammonium persulfate as the oxidant and BC as the template. The resultant PANI/BC nanocomposite membranes were characterized by Fourier transform infrared spectroscopy (FTIR), field-emission scanning electron microscopy (FESEM), thermogravimetric analysis (TGA), and electrical conductivity and mechanical measurements. The influence of various reaction times, various acids serving as dopants, and the content of PANI of composites on the properties of the composites was also investigated.

## EXPERIMENTAL SECTION

**Materials.** The BC membrane was kindly provided by Hainan Yeguo Foods Co. Ltd. The membrane was washed with distilled

**Received:** May 12, 2011

**Revised:** May 26, 2011

**Published:** June 14, 2011

water and treated with 1% sodium hydroxide at 80 °C for 1 h, followed by rinsing with water. The other chemicals were purchased from Shanghai Chemical Company and were used as received without any further purification.

#### Preparation of the PANI/BC Nanocomposite Membrane.

Water-wet samples in small pieces (containing about 50 mg of dry BC each piece) were dried for 2 h at 80 °C. The sample was then placed in a 500 mL three-necked flask fitted with a mechanical stirrer containing a mixture of 250 mL of 2.0 mol/L HCl solution dissolving 0.2 mol aniline monomers. After the cellulose was stirred for 1 h, 2.0 mol/L ammonium persulfate aqueous solution was added dropwise. The mixture was stirred in an ice bath for 30, 60, 90, 120, and 180 min, respectively. Different kinds of acids were used to substitute HCl, including 250 mL of 2.0 mol/L *p*-toluenesulfonic acid (*p*-TSA), dodecylbenzene sulfonic acid (DBSA), or  $\text{NH}_2\text{SO}_3\text{H}$  and 125 mL of 2.0 mol/L  $\text{H}_2\text{SO}_4$  or  $\text{H}_3\text{PO}_4$ . At the end of each experiment, the obtained product was washed thoroughly with 75% (v/v) alcohol followed by distilled water to remove the byproducts and remaining reagents. Then the samples were dried in a vacuum oven at 60 °C to constant weight.

**Characterization.** The content of PANI was calculated based on the weight increment of the BC membrane. The morphologies of PANI/BC nanocomposite membranes were characterized using an S-4800 field emission scanning electron microscope. Prior to analysis, samples were cut into small pieces from the prepared sample and coated with a thin layer of evaporated gold. The infrared spectra were recorded on a Nicolet NEXUS-670 FT-IR. Each sample was grounded with dried potassium bromide (KBr) powder and compressed into a disk and then was subjected to analysis. Thermal gravimetric (TG) curves were obtained for dried samples in Universal V3.8B equipment from TA-Instruments. Samples were heated in open alumina pans from 30 to 800 °C, under a nitrogen atmosphere, at a heating rate of 10 °C/min. Tensile strengths of both BC and PANI/BC membranes were measured using a WDW 3020 Universal Testing Machine at room temperature and with a speed of 5 mm/min. Elongation at break and Young's modulus of these samples were, therefore, measured. Samples 30 mm in length, 5 mm in width, and 0.03 mm in thickness were used in these measurements. The electrical conductivity of the composites was measured at room temperature by the standard four-probe method.

## RESULTS AND DISCUSSION

The flexible nanoporous BC membranes with 0.03 mm thickness were used to synthesize composite membranes. The aniline hydrochloride could permeate through the inner network of BC. At the same time, the large amount of hydroxyl groups of BC could interact with amine groups of aniline to form the hydrogen bonds which ensure the uniform distribution of aniline on the surface of BC nanofibers. After being immersed in the oxidant solution, the aniline monomer would polymerize in the network of BC, as illustrated in Figure 1. Figure 2 shows the images of the original BC membrane and the PANI/BC composite membrane containing 10.7 wt % PANI. Compared with the BC membrane, the composite membrane showed an obvious dark green color, which revealed the successful incorporation of PANI in the BC membrane. In addition, they are rather flexible to be curled which can be seen from Figure 2b.

The FTIR spectra of BC, PANI, and PANI/BC composite samples are shown in Figure 3. The bands at 3410, 2900, 1642,

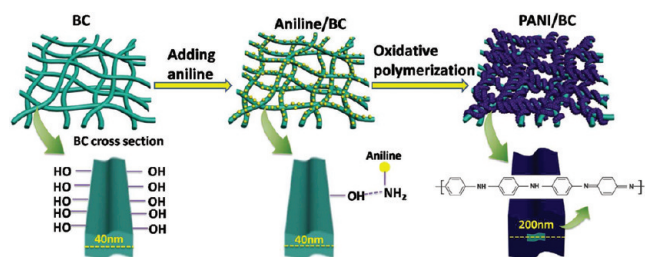


Figure 1. Schematic diagram of the formation of PANI/BC nanocomposites.

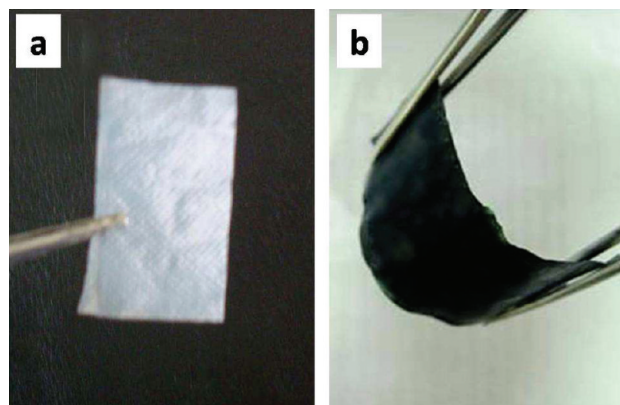


Figure 2. Optical images of the (a) pure BC membrane and (b) PANI/BC composite membrane (10.7 wt % PANI).

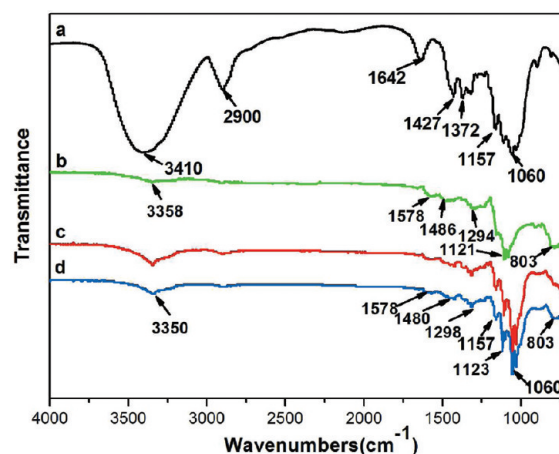
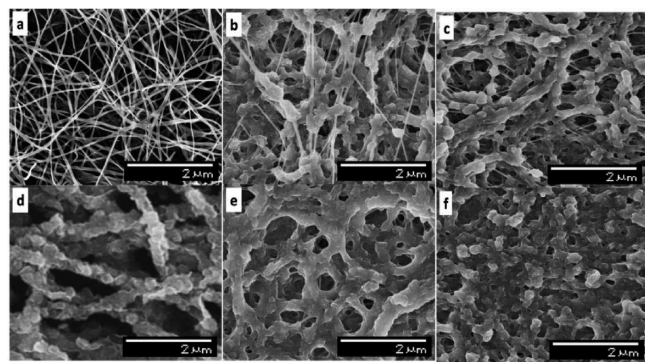


Figure 3. FTIR spectra of (a) pure BC, (b) PANI, (c) PANI/BC nanocomposite with 5.8 wt % PANI, and (d) PANI/BC nanocomposite with 10.7 wt % PANI, respectively.

1427, 1372, 1157, and 1060  $\text{cm}^{-1}$  in Figure 3a are associated with native BC.<sup>19</sup> A strong band at 3410  $\text{cm}^{-1}$  arises from the stretching of hydroxyl groups. The bands at 2900 and 1642  $\text{cm}^{-1}$  originate from the C–H stretching and the H–O–H bending of the absorbed water, respectively. The peak at 1372  $\text{cm}^{-1}$  is attributed to the O–H bending, and that at 1157  $\text{cm}^{-1}$  corresponds to the C–O antisymmetric bridge stretching. A strong band at 1060  $\text{cm}^{-1}$  is due to the C–O–C pyranose ring skeletal vibration. The typical feature of pure PANI is also seen in Figure 3b. The peak at 803  $\text{cm}^{-1}$  corresponding to the out-of-plane bending vibration of the C–H band of *p*-disubstituted





**Figure 4.** FE-SEM images of (a) pure BC and the PANI/BC composites formed with the reaction time of (b) 30 min, (c) 60 min, (d) 90 min, (e) 120 min, and (f) 180 min, respectively.

benzene ring appears. The peaks at 1294 and 1121  $\text{cm}^{-1}$  due to the stretching of the C–N band and vibration of C–H in the benzene ring have been observed. The peaks around 1486 and 1578  $\text{cm}^{-1}$  are assigned to stretching vibration of N–B–N and N=Q=N structures, respectively (B and Q represent benzenoid and quinoid moieties in the PANI chains).

Figure 3c and d show the spectra of the PANI/BC composites. Compared with the spectra of pure BC, it was found that the absorption peak at 3410  $\text{cm}^{-1}$  in the spectrum of BC is shifted to 3350  $\text{cm}^{-1}$  in the spectrum of the BC/PANI composite. Furthermore, the absorption intensity of the band in the BC/PANI membrane became weaker with increasing content of PANI. These phenomena indicated that the bacterial cellulose is successfully activated by acids and the intermolecular hydrogen bands are broken.<sup>20</sup> So more hydroxyl groups become accessible which helps to form the uniform dispersion of PANI in the nanofibrous membrane, and the result will be confirmed in the section of SEM.

The morphologies of BC and PANI/BC composites were studied using FE-SEM. Figure 4a shows the FE-SEM images of freeze-dried BC samples. The BC membrane consists of continuous nanofibers with a diameter in the range from 20 to 60 nm to form an ultrafine network structure. Figure 4b–f shows FE-SEM images of PANI/BC composites formed with different reaction times. When the reaction time is 30 min, some disconnected PANI particles appear on the BC nanofibers. As the reaction proceeds, it is found that the PANI nanoparticles deposited on the surface of fibers connected to form a continuous nanosheath with the diameter around 200 nm by taking along cellulose templates. The hydrogen bands between hydroxyl groups of BC and amine groups of aniline might serve as a traction force to assist the growing of the continuous nanosheath of PANI over cellulose and avoid the large-scale aggregate formation. It is observed that PANI particles deposited on the surface of the BC nanofibers with little PANI aggregates especially in the optimized reaction condition (Figure 4d). This demonstrated that the nanofibrils work as a good template for polymerization. Some similar nanostructures have been presented earlier by polymerizing conducting polymers onto cellulose nanofibrils. Mihranyan et al. have shown similar results for polymerization of the conducting polymer polypyrrole onto crystalline cellulose fibers from the green algae *Cladophora*.<sup>21</sup> In addition, Nyström et al. have shown that polypyrrole can be deposited in a similar manner onto nanofibrils from wood.<sup>22</sup>

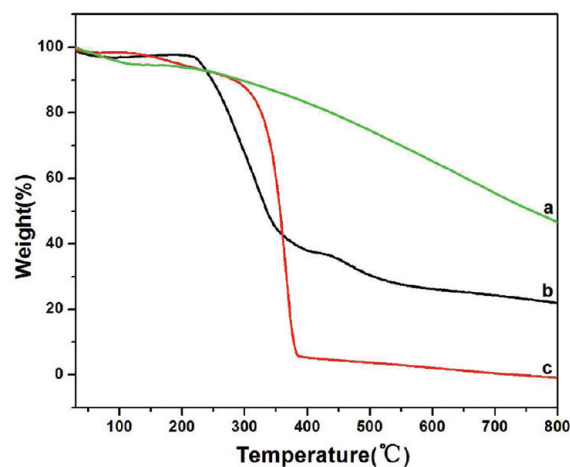


**Figure 5.** TG curves of (a) PANI (doped by HCl), (b) the PANI/BC composite with 10.7 wt % PANI (doped by HCl), and (c) pure BC.

**Table 1.** Effects of Reaction Time on the Content of PANI and the Electrical Conductivity of PANI/BC Composites

reaction time (min)	content of PANI (wt %)	electrical conductivity (S/cm)
30	5.8	$2.0 \times 10^{-4}$
60	9.1	$4.7 \times 10^{-3}$
90	10.7	$5.0 \times 10^{-2}$
120	13.1	$2.3 \times 10^{-3}$
180	15.3	$9.5 \times 10^{-3}$

While further increasing the reaction time, the content of PANI particles increases with the precipitation or aggregation forming on the surface of BC membranes (Figure 4e and f).

We have investigated the thermal property of the PANI/BC composite with 10.7 wt % PANI shown in Figure 5b. The TG curves of pure PANI and BC in Figure 5a and c are also shown for comparison. As shown in Figure 5, the TG curve of the PANI/BC composite can be distinctly divided into three stages. During the initial stage from room temperature to 100 °C, the moisture present in the composite vaporized. From 216 to 425 °C, the samples experienced a sharp weight loss, which might be ascribed to the destruction of the crystalline region of BC and decomposition of amorphous BC into a monomer of D-glucopyranose and further into a free radical. The TG curve of pure BC indicates that it also experiences a similar weight loss process. However, it can be seen from the curves that the onset temperature of the thermo-oxidative degradation of the BC membrane is 80 °C lower than PANI/BC, indicating that the thermal stability of the PANI/BC composite is higher than that of untreated BC. At the same time, the massive weight loss of the BC membrane happens at the higher temperature which is 78 °C higher than PANI/BC, which may be due to the weakened inter- and intramolecular hydrogen bonding of BC in the PANI/BC composite. The final step in weight loss is observed from 425 to 800 °C which is attributed to the thermal-oxidative degradation of PANI. The phenomenon is in accordance with the result obtained by Mo et al. and Stejskal et al.<sup>20,23</sup>

Table 1 lists the effects of the reaction time on the content of PANI and the electrical conductivity of PANI/BC composites. The reaction time of polymerization of aniline was 30, 60, 90,

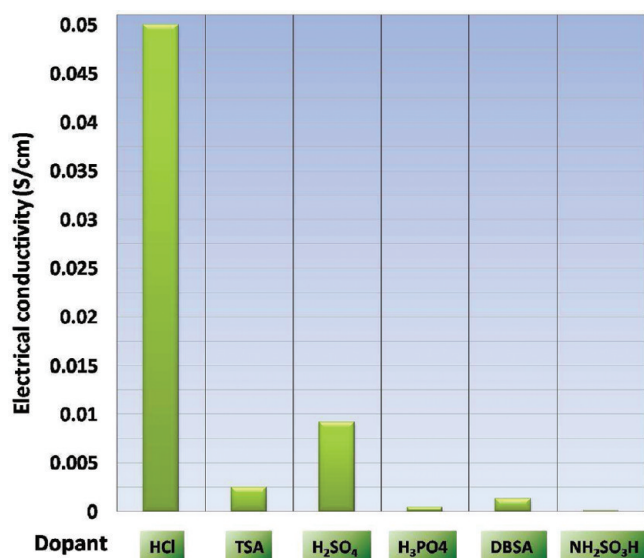


Figure 6. Effect of different types of acids (2.0 mol/L) on the electrical conductivity of PANI/BC composite membranes.

120, and 180 min, respectively. The result shows that the amount of anilines deposited on the surface of cellulose increases with the increase of the reaction time. A general trend of initial increase and subsequent decrease in electrical conductivity of BC/PANI composites with increasing reaction time can be seen in Table 1. The initial increase may be due to that the disconnected PANI nanoparticles gradually grow into a continuous nanosheath by taking along the BC templates with longer reaction time, leading to the optimum conductivity. The conductivity reached the maximum  $5.0 \times 10^{-2}$  S/cm when the reaction time was 90 min. However, too long reaction time leads to the precipitate or aggregate of PANI particles and excessive oxidation of the aniline monomer with the fracture of the PANI conjugated chain. At the same time, the doping system may be undermined to some extent, and the insoluble polyaniline may generate in the composite membranes which result in the decrease of the conductive component, thus reducing the corresponding conductivity of composite films.

It is believed that the electrical conductivity of PANI/BC composites is influenced by the type of dopant used. Higher conductivity could be obtained when PANI is doped by stronger protonic acids.<sup>24</sup> In this paper, the influence of the different types of acids on the electrical conductivity of the PANI/BC composites is investigated. As shown in Figure 6, the conductivity of the prepared composites is greatly different when different acids were used. The higher acidity increased the electrical conductivity of the composite membranes except for the condition of H<sub>2</sub>SO<sub>4</sub>. This may be due to the fact that the stronger acid usually could offer enough protonic hydrogen with the higher degree of ionization, which assures the favorable electrical conductivity of the doped PANI with the same concentration of the acid and oxidant. However, H<sub>2</sub>SO<sub>4</sub> cannot ionize completely, and hydrogen sulfate anions are exclusively present in PANI/H<sub>2</sub>SO<sub>4</sub>.<sup>25</sup> So, the conductivity of PANI doped by H<sub>2</sub>SO<sub>4</sub> is slightly lower than that of HCl. The electrical conductivities as high as  $10^{-2}$  S/cm were obtained for the PANI/BC nanocomposite membranes, which are at least 1 order of magnitude higher than previously reported work for PANI/cellulose films.<sup>20</sup>

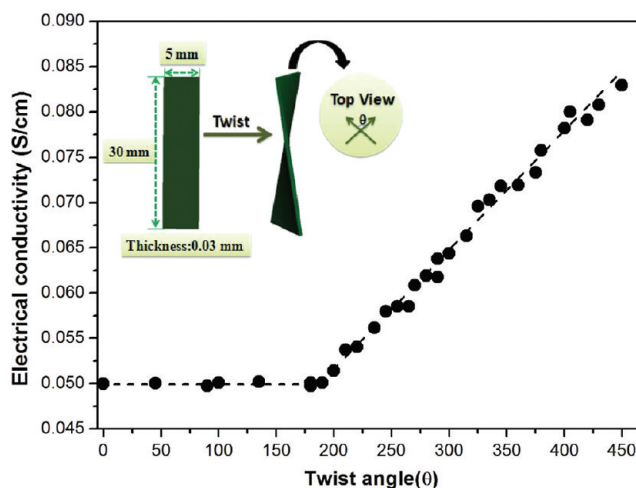


Figure 7. Conductivity of PANI/BC composite membranes with 10.7 wt % PANI as a function of twist angle ( $\theta$ ). The inset shows the sample size and twist of the composite membrane.

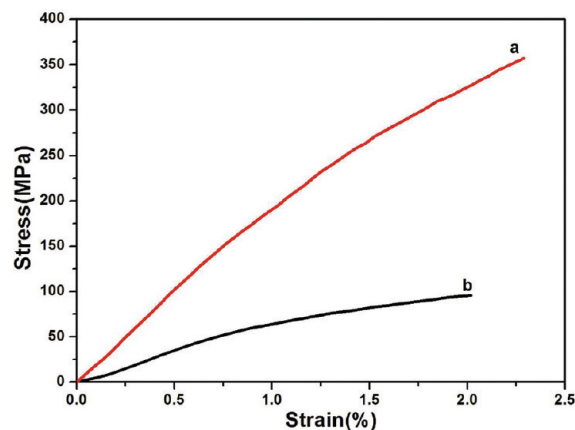


Figure 8. Tensile stress–strain behaviors of (a) air-dried BC and (b) PANI/BC composite membranes with 10.7 wt % PANI.

The relation between conductivity and the angle of twist for the composite membrane is shown in Figure 7. The electrical conductivity is found to be nearly invariant when the angles of twist are below  $200^\circ$ . However, when further increasing the angle, the conductivity of the composite almost linearly increases. The conductivity increases by 1.6 times when the angle of twist is  $450^\circ$ . A similar phenomenon is observed with PANI/pulp composite fibers, which may be due to the improved electronic contact between individual fibers in the membranes with denser networks brought by the mechanical pressure.<sup>26</sup> The sensitivity of the electrical conductivity PANI/BC membranes to the strain could be applied to strain sensors.

To investigate the mechanical characteristics of PANI/BC membranes, the tensile test was performed. The tensile behavior of native BC and PANI/BC membranes is shown in Figure 8. The Young's modulus and tensile strength of BC are 20.8 GPa and 357.3 MPa, respectively, while the Young's modulus of the PANI/BC membrane with 10.7 wt % PANI is around 5.6 GPa and tensile strength around 95.7 MPa. This decreased behavior of PANI/BC membranes might be associated with the weakened inter- and intramolecular hydrogen bonding of BC caused by the

introduction of PANI. It is obvious that the nanocomposites combine the excellent mechanical properties of the BC membrane and the conductive properties of the PANI. In a word, the PANI/BC composites are present with favorable conductivity and good mechanical property which can be used as a promising material in the application of sensors, flexible electrodes, display devices, and other electrically conductive flexible film fields.

## CONCLUSIONS

The novel conductive PANI/BC nanocomposite membranes have been successfully synthesized in situ by oxidative polymerization of aniline using BC as the template. It is found that the PANI particles uniformly deposited on the surface of BC connected to form a continuous nanosheath by taking along the BC template, which greatly increases the thermal stability of BC. FTIR spectra indicated that BC is successfully activated by acids, and the intermolecular hydrogen bands are broken, which helps to form the uniform dispersion of PANI in the nanofibrous membrane. The electrical conductivity can achieve  $5.0 \times 10^{-2}$  S/m by controlling the reaction time and the proton acids used. In addition, the conductivity of the composite membrane increases almost linearly when the angles of twist are above  $200^\circ$ . The composites exhibit excellent flexibility and good mechanical properties with the Young's modulus of 5.6 GPa and tensile strength of 95.7 MPa. The nanocomposites synergistically combine the electronic characteristics of PANI with the outstanding mechanical characteristics of the BC matrix. This work would provide a straightforward method to prepare flexible films with high conductivity and good mechanical properties which could be applied in sensors, flexible electrodes, and flexible displays. It also opens a new field of potential applications of BC materials.

## AUTHOR INFORMATION

### Corresponding Author

\*Tel.: +86-21-67792958. Fax: +86-21-67792726. E-mail: chensy@dhru.edu.cn; wanghp@dhru.edu.cn.

## ACKNOWLEDGMENT

The authors thank Hainan Yeguo Foods Co. Ltd for supplying BC samples. This work was financially supported by Doctoral Fund of Ministry of Education of China (20090075120011), Program of Introducing Talents of Discipline to Universities (B07024), Shanghai Leading Academic Discipline Project (B603), The National Natural Science Foundation of China (51003012), Project of the Action on Scientists and Engineers to Serve Enterprises (2009GJE20016), and the Innovation Funds for Ph. D Students (Weili Hu) of Donghua University.

## REFERENCES

- (1) Kaiser, A. A.; Hyland, M. M.; Patterson, D. A. *J. Phys. Chem. B* **2009**, *113*, 14986–14993.
- (2) Guimard, N. K.; Gomez, N.; Schmidt, C. E. *Prog. Polym. Sci.* **2007**, *32*, 876–921.
- (3) Bai, H.; Chen, Q.; Li, C.; Lu, C. H.; Shi, G. Q. *Polymer* **2007**, *48*, 4015–4016.
- (4) Hong, S. F.; Hwang, S. C.; Chen, L. C. *Electrochim. Acta* **2008**, *53*, 6215–6227.
- (5) Amrithesh, M.; Aravind, S.; Jayalekshmi, S.; Jayasree, R. S. *J. Alloys Compd.* **2008**, *449*, 176–179.
- (6) Prabhakar, N.; Arora, K.; Singh, H.; Malhotra, B. D. *J. Phys. Chem. B* **2008**, *112*, 4808–4816.

- (7) Lange, U.; Roznyatouskaya, N. V.; Mirsky, V. M. *Anal. Chim. Acta* **2008**, *614*, 1–26.
- (8) Cerqueira, D. A.; Valente, A. J. M.; Filho, G. R.; Burrows, H. D. *Carbohydr. Polym.* **2009**, *78*, 402–408.
- (9) Chandran, A. S.; Narayanankutty, S. K. *Eur. Polym. J.* **2008**, *44*, 2418–2429.
- (10) Lakshmi, K.; John, H.; Mathew, K. T.; Joseph, R.; George, K. E. *Acta Mater.* **2009**, *57*, 371–375.
- (11) Jeevananda, T.; Siddaramaiah. *Eur. Polym. J.* **2003**, *39*, S69–S78.
- (12) Nyholm, L.; Nyström, G.; Mihranyan, A.; Strømme, M. *Adv. Mater.* **2011** 10.1002/adma.201004134.
- (13) Cerqueira, D. A.; Valente, A. J. M.; Filho, G. R.; Burrows, H. D. *Carbohydr. Polym.* **2009**, *78*, 402–408.
- (14) Gelin, K.; Bodin, A.; Gatenholm, P.; Mihranyan, A.; Edwards, K.; Strømme, M. *Polymer* **2007**, *48*, 7623–7631.
- (15) Hu, W.; Chen, S.; Xu, Q.; Wang, H. *Carbohydr. Polym.* **2011**, *83*, 1575–1581.
- (16) Gindl, W.; Keckes, J. *Compos. Sci. Technol.* **2004**, *64*, 2407–2413.
- (17) Yano, H.; Sugiyama, J.; Nakagaito, A. N.; Nogi, M.; Matsuura, T.; Hikita, M.; Handa, K. *Adv. Mater.* **2005**, *17*, 153–155.
- (18) Nakagaito, A. N.; Iwamoto, S.; Yano, H. *Appl. Phys. A: Mater. Sci. Process.* **2005**, *80*, 93–97.
- (19) Hu, W.; Liu, S.; Chen, S.; Wang, H. *Cellulose* **2011**, *18*, 655–661.
- (20) Mo, Z.; Zhao, Z.; Chen, H.; Niu, G.; Shi, H. *Carbohydr. Polym.* **2009**, *75*, 660–664.
- (21) Mihranyan, A.; Nyholm, L.; Garcia Bennett, A. E.; Strømme, M. *J. Phys. Chem. B* **2008**, *112*, 12249–12255.
- (22) Nyström, G.; Mihranyan, A.; Razaq, A.; Lindström, T.; Nyholm, L.; Strømme, M. *J. Phys. Chem. B* **2010**, *114*, 4178–4182.
- (23) Stejskal, A.; Trchova, M.; Sapurina, I. *J. Appl. Polym. Sci.* **2005**, *98*, 2347–2354.
- (24) Mattoso, L. H.; Medeiros, E. S.; Baker, D. A.; Avloni, J.; Wood, D. F.; Orts, W. J. *J. Nanosci. Nanotechnol.* **2009**, *9*, 2917–2922.
- (25) Gemeay, A. H.; Mansour, I. A.; El-Sharkawy, R. G.; Zaki, A. B. *Eur. Polym. J.* **2005**, *41*, 2578–2583.
- (26) Goto, H. *Text. Res. J.* **2011**, *81*, 122–127.